Effects of Asp-96 → Asn, Asp-85 → Asn, and Arg-82 → Gln Single-Site Substitutions on the Photocycle of Bacteriorhodopsin†

Thorgeir E. Thorgeirsson,‡ Steven J. Milder,‡,§ Larry J. W. Miercke,∥ Mary C. Betlach,∥ Richard F. Shand,∥,⊥ Robert M. Stroud,∥ and David S. Kliger*,‡

Department of Chemistry and Biochemistry, University of California, Santa Cruz, California 95064, and Department of Biochemistry and Biophysics, University of California, San Francisco, California 94143

Received January 18, 1991; Revised Manuscript Received May 7, 1991

ABSTRACT: Bacteriorhodopsin (BR) with the single-site substitutions Arg-82 → Gln (R82Q), Asp-85 → Asn (D85N), and Asp-96 → Asn (D96N) is studied with time-resolved absorption spectroscopy in the time regime from nanoseconds to seconds. Time-resolved spectra are analyzed globally by using multiexponential fitting of the data at multiple wavelengths and times. The photocycle kinetics for BR purified from each mutant are determined for micellar solutions in two detergents, nonyl glucoside and CHAPSO, and are compared to results from studies on delipidated BR (d-BR) in the same detergents. D85N has a red-shifted ground-state absorption spectrum, and the formation of an M intermediate is not observed. R82Q undergoes a pH-dependent transition between a purple and a blue form with different pK_a values in the two detergents. The blue form has a photocycle resembling that for D85N, while the purple form of R82Q forms an M intermediate that decays more rapidly than in d-BR. The purple form of R82Q does not light-adapt to the same extent as d-BR, and the spectral changes in the photocycle suggest that the light-adapted purple form of R82Q contains *all-trans*- and 13-*cis*-retinal in approximately equal proportions. These results are consistent with the suggestions of others for the roles of Arg-82 and Asp-85 in the photocycle of BR, but results for D96N suggest a more complex role for Asp-96 than previously suggested. In nonyl glucoside, the apparent decay of the M-intermediate is slower in D96N than in d-BR, and the M decay shows biphasic kinetics. However, the role of Asp-96 is not limited to the later steps of the photocycle. In D96N, the decay of the KL intermediate is accelerated, and the rise of the M intermediate has an additional slow phase not observed in the kinetics of d-BR. The results suggest that Asp-96 may play a role in regulating the structure of BR and how it changes during the photocycle.

Bacteriorhodopsin (BR)[1] is an integral membrane protein found in the purple membrane (PM) of *Halobacterium halobium*. BR contains a retinal chromophore that is connected to the protein through a Schiff base linkage to lysine-216. Absorption of light by BR activates a photocycle whose function is to pump protons from the interior to the exterior side of the bacterium cell membrane. This generates an electrochemical gradient that the organism uses to drive energy-requiring processes (Stoeckenius & Bogomolni, 1982). The initial step in the photocycle is the photoisomerization of the *all-trans*-retinal group to a 13-cis configuration (Ottolenghi, 1982; Mathies et al., 1988). The protein then undergoes a series of conformational changes, with at least six intermediates (K → KL → L → M → N → O → BR) that can be identified by their spectral characteristics (Lozier et al., 1975; Ottolenghi, 1982; Milder & Kliger, 1988). There is still some dispute about the details of the photocycle, but recent studies support the view that a sequential pathway with back-reactions between the intermediates can adequately account for the observed complexities in the kinetics (Varo & Lanyi, 1990; Ames & Mathies, 1990; Chernavskii et al., 1989).

The retinal Schiff base deprotonates when M is formed and is reprotonated with the formation of N (Fodor et al., 1988). Reisomerization of the chromophore to the all-trans conformation takes place upon the formation of O (Smith et al., 1983). The changes in the protonation of the chromophore have been suggested to be directly involved in the transfer of the proton across the membrane, with the chromophore acting as a light-activated switch connecting proton-transfer pathways within the protein.

Low-temperature FTIR measurements have shown that changes in the protonation states of aspartic acid and tyrosine residues in the protein are coupled to the changes in the chromophore (Eisenstein et al., 1987; Rothschild et al., 1988). Further studies on BRs with site-specific substitutions have shown that these residues are tyrosine-185 (Braiman et al., 1988a; Rothschild et al., 1990; Duñach et al., 1990) and aspartic acids-85, -96, and -212 (Braiman et al., 1988b; Gerwert et al., 1989). Recent models for the structure of BR (Henderson et al., 1990) along with studies of BR and of BR from mutants have identified the amino acid residues that are most likely to interact directly with the Schiff base. It has been proposed that the negatively charged Asp-85 and Asp-212 along with the positively charged Arg-82 form a complex counterion to the protonated Schiff base of retinal in BR

† This work was supported by the National Institutes of Health through Grants EY00983 (D.S.K.), GM32079 (R.M.S.), and GM31785 (M.C.B.).

* Author to whom correspondence should be addressed.

‡ University of California, Santa Cruz.

§ Present address: Division of Natural Sciences, The Evergreen State College, Olympia, WA 98505.

∥ University of California, San Francisco.

⊥ Present address: Department of Biological Sciences, Northern Arizona University, Flagstaff, AZ 86011.

[1] Abbreviations: BR, bacteriorhodopsin; DA, dark-adapted; d-BR, delipidated BR monomers; e-BR, bacteriorhodopsin monomers prepared as an expressed fusion protein in *E. coli*; CHAPSO, 16 mM 3-[(3-(cholamidopropyl)dimethylammonio]-2-hydroxy-1-propanesulfonate; LA, light-adapted; NG, 18 mM nonyl β-D-glucopyranoside; PM, purple membrane; SVD, singular value decomposition.

0006-2960/91/0430-9133$02.50/0

(Ames et al., 1990; Braiman et al., 1988b; Henderson et al., 1990; Lin & Mathies, 1989). Whether these and/or other residues in BR form a proton wire that moves the proton to and from the Schiff base and across the protein during the photocycle is of great current interest.

Herein we report studies on the photocycle of three BRs, each containing a single site-specific substitution. Each of the replaced residues has been shown to be integral to the function of the light-driven proton pump in BR. Since spectra are recorded with a time resolution of 10 ns, our results provide an opportunity to investigate the effects that these mutations have on all of the steps of the photocycle that follow the formation of the KL intermediate. The global analysis approach used in this study allows us to calculate putative spectra for the intermediates and is more sensitive to subtle effects, like small spectral shifts, than methods using a single-wavelength approach.

Experimental Procedures

Preparation of Protein Samples. PM from *H. halobium* (strain JW-3) was provided by Walther Stoeckenius of UCSF. d-BR/CHAPSO (16.4 mM CHAPSO) in buffer A (100 mM NaCl/20 mM acetate, pH 5) was made as described previously (Miercke et al., 1989), and d-BR/NG (18 mM NG) in buffer A was prepared by dye–ligand affinity chromatography (Miercke et al., 1991). Expression of bacterioopsin in *Escherichia coli* as a fusion protein (i.e., e-BR) and site-directed mutagenesis are described by Shand et al. (1991). Three e-BRs with single amino acid substitutions, Asp-85 → Asn, Asp-96 → Asn, and Arg-82 → Gln, were prepared in CHAPSO or NG according to Miercke et al. (1991). The purified BR samples have dark-adapted absorbance ratios ($A_{280}/A_{\lambda_{max}}$) of 1.5 and 1.5–2.1 in NG and CHAPSO, respectively. Flash photolysis studies were performed on samples from site-directed mutants at the same detergent concentrations as for d-BR in buffer A. For studies on the effect of pH on the photocycle, the solution was made 4 mM in phosphate and titrated to the desired pH by slowly adding a solution of either NaOH or HCl.

Photocycle Measurements and Kinetic Analysis. Photocycle measurements were made by using the same laser photolysis apparatus used in our study on monomeric BR in various detergents (Milder et al., 1991). The photocycle is initiated with a 532-nm light pulse (2 mJ, 7 ns FWHM) from a Quanta Ray DCR2 Nd:YAG laser. The probe light comes from an EG&G Q3CP-2 xenon flashlamp (τ = 5 μs), and light intensities were measured by using a gated optical multichannel analyzer (OMA). The excitation and probe beams entered the sample at an angle of 90° to one another, and the excitation light was polarized at the magic angle (54.7°) relative to the probe beam polarization to eliminate photoselection artifacts resulting from protein rotation. The laser excited a sample volume of 2 × 10 × 1 mm. The actinic path length was 2 mm, the probe path length was 10 mm, and the sample had an optical density between 0.7 and 1 at the wavelength of maximum absorption. At each time at which transient spectra were measured, 24–36 spectra were recorded and averaged. For each time, a fresh aliquot of sample was used and light-adapted before data collection. For each sample, the repetition rate of the laser excitation was slow enough to ensure completion of the photocycle between excitation pulses. Temporal information is obtained by gating the OMA with a 10-ns pulse from a PAR 1302 pulser at various delays after laser excitation. Transient difference spectra were calculated by taking the log of the ratio of the probe signal without and with photolysis of the sample. The data from the OMA consist of ΔOD values at 640 different wavelengths between 350 and 750 nm, but this number was reduced to 160 by averaging over each set of 4 consecutive channels, yielding a spectral resolution of 2 nm. Transient difference spectra were collected at 25–40 different times after photolysis, with a minimum of 3 times per decade.

To obtain a difference spectrum, 150 μL of sample was placed in a fluorescence cuvette inside a thermostated sample holder (20.5 ± 0.5 °C) and light-adapted at a light flux of 0.2 W/cm^2, using a 150-W Cole Parmer quartz–halogen lamp whose output had been filtered with a heat-absorbing filter and a Corning 3-69 (450-nm cutoff) glass filter. For d-BR, illumination for 1 min ensured full light-adaptation under our conditions, as no evidence for a red-absorbing transient (C_{610}) in the time regime between 10 μs and 1 ms after excitation was observed, and further illumination led to no further red shift in the light-adapted ground-state spectrum. Some of the mutant samples were more light-sensitive than d-BR. Thus, for each series of time-resolved difference spectra, care was taken to light-adapt all the samples for the same length of time. Dark adaptation rates depend on which detergent is used (Milder et al., 1991). In NG, the dark adaptation rates are relatively fast, and we maintained a low light flux (0.04 W/cm^2) on the sample during data collection. This prevented the return of BR to the 13-cis form and assured complete light adaptation such that our samples contained less than 10% of 13-*cis*-BR. Again, this was checked by noting the absence of a C_{610} transient in the d-BR and D96N samples. For samples in CHAPSO, no background illumination was required after the initial light adaptation.

Singular Value Decomposition and Nonlinear Exponential Fitting. Time-resolved spectra were analyzed globally at all times and wavelengths simultaneously. The analysis was done on IBM compatible personal computers (80386/80387 4 Mb memory and 80386/80287 1 Mb memory) using singular value decomposition (SVD) and global exponential fitting routines from the Matlab (The Math Works) software package (Hug et al., 1990). First, the entire set of data from an experiment is subjected to SVD. This process gives orthonormal basis spectra that can be used to represent the entire data set using far fewer spectra because the transient difference spectra contain redundant spectral information. The data matrix can be written as a product of three matrices:

$$\Delta OD(\lambda,t) = \mathbf{USV}' \quad (1)$$

where $\mathbf{V}'$ stands for the transpose of $\mathbf{V}$. The matrix $\mathbf{U}$ contains the orthonormal basis spectra, $\mathbf{S}$ the associated eigenvalues, and $\mathbf{V}$ the time evolution of the spectra. The square of the difference between the actual data and data calculated from eq 1 by using the o most important basis spectra is

$$\sum_{\lambda}\sum_{\text{times}} [\Delta OD - \mathbf{U}_o\mathbf{S}_o\mathbf{V}'_o]^2 = \sum_{i>o}^{n}\mathbf{S}_{ii}^2 \quad (2)$$

where $\mathbf{S}_{ii}$ are the singular values, or the diagonal elements of $\mathbf{S}$. The significance of each basis spectrum is thus proportional to the square of its singular value, and the data set is adequately represented by a truncated set when the result of eq 2 is within the noise level in the experiment. The significant basis spectra are then used in a nonlinear least-squares (simplex) routine to fit the data to a sum of exponentials:

$$\Delta OD(\lambda,t) = \sum_{i=0}^{n}\mathbf{b}_i(\lambda)e^{-k_i t} \quad (3)$$

where n is the number of exponentials, k_i are the observed rate constants, and $\mathbf{b}_i(\lambda)$ are the "b-spectra" that are associated

with the apparent rates. Equation 3 contains a constant term ($i = 0$, $k_0 = 0$) that consists of all photoproducts that appear stable on the time scale of the experiment. The simplex fit minimizes the sum of squared residuals between the fit and the data. The input parameters are the number of rate constants and their initial values. The use of SVD mainly serves the purpose of reducing computational time. We ensured that the result did not depend on the number of basis spectra used by including a sufficiently large number of them. The main criterion for a good fit is a low value for the sum of squared residuals. A good fit also has residuals that are free from spectral structure. For a detailed discussion of this method, see Hug et al. (1990), Nagle et al. (1982), and Xie et al. (1987).

Calculation of Intermediate Spectra. The interpretation of the b-spectra is dependent on the model used to represent the process under study, since the b-spectra simply describe the spectral changes according to eq 3. Once the nonlinear fit has been performed, the apparent rates and the b-spectra obtained can be used to calculate a difference spectrum for any delay following photolysis using eq 3. Each b-spectrum is multiplied with the appropriate time-dependent exponential factor, and the resulting sum gives the transient difference spectrum at any given time. In the case of a purely parallel decay mechanism, each b-spectrum represents the actual difference spectrum between each pair of states. It is also fairly straightforward to calculate the actual intermediate spectra when intermediates form and decay according to a simple sequential scheme without back-reactions (Nagle et al., 1982). Then the observed rate constants are equal to the microscopic rate constants. Intermediate spectra can be calculated as linear combinations of the b-spectra in more complicated cases when the underlying first-order mechanism is known. Since the actual mechanism of the photocycle of BR is still a matter of debate, we have chosen, in presenting our results here, to calculate putative spectra for the intermediates assuming a simple sequential photocycle without back-reactions. If the nonlinear fit is consistent with n apparent rates, $n + 1$ spectra will be obtained. Each spectrum will contain a negative contribution from the amount of light-adapted BR that undergoes the photocycle. This contribution is the same for all the spectra, and so the same scaled spectrum of light-adapted BR is added to all the calculated spectra. The scaling factor is estimated by using the criteria that each intermediate spectrum has to be nonnegative at all wavelengths and that they each must have a log-normal shape. In all cases presented here, we have used a factor just high enough to ensure nonnegative optical densities at all wavelengths. This method of presenting the data only works when the photocycle can to some degree be approximated by a simple sequential scheme, and the resulting spectra have to be interpreted with this approximation in mind. Intermediate spectra will appear bimodal in this approach when equilibria exist between successive intermediates.

Results and Discussion

Time-resolved difference spectra for d-BR and the e-BRs with single amino acid substitutions were measured in the two detergents. d-BR is BR grown in *H. halobium*, delipidated, and detergent-solubilized in either CHAPSO or NG. Control experiments were carried out on three other nonmutant monomeric preparations: e-BR, w-BR, and p-BR. e-BR is prepared from *E. coli* as a fusion protein containing 13 heterologous amino acids at the amino terminus (Shand et al., 1991). w-BR is d-BR that has been denatured and subsequently renatured in the same way as e-BR and e-BR variants

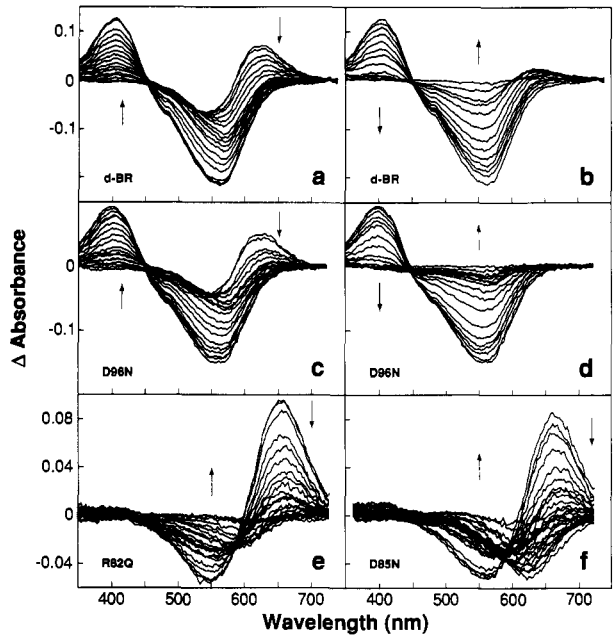

FIGURE 1: Transient difference spectra obtained for d-BR and preparations from mutants in NG after excitation at 532 nm with a 2-mJ, 7-ns laser pulse. (a) Short time data showing rise of the M intermediate for d-BR/NG ($OD_{max} = 0.78$). Times after excitation: 50, 100, 250, 350, 500, and 750 ns; 1, 1.5, 2, 3, 4, 5, 7.5, 10, 15, 25, 35, 50, and 100 μs. (b) Long time data showing decay of M and return to BR. Times after excitation: 50, 100, 250, and 500 μs; 1, 1.5, 2, 3, 5, 7.5, 10, 20, and 40 ms. (c) Short time data for D96N/NG ($OD_{max} = 0.65$) showing decay of the KL intermediate and rise of the M intermediate. Times after excitation: 50, 100, 250, 350, 500, and 750 ns; 1, 1.5, 2, 3, 5, 7.5, 10, 15, 25, 35, 50, and 100 μs. (d) Decay of M and return to BR for D96N/NG. Times after excitation: 250, 450, and 750 μs; 1, 1.5, 2, 3, 5, 7.5, 10, 15, 20, 30, 40, 60, 80, 160, and 360 ms. (e) Data for R82Q/NG ($OD_{max} = 0.67$). Times after excitation: 35, 50, 100, 250, 500, and 750 ns; 1, 1.5, 3, 4, 7, 10, 50, 100, 170, 250, and 750 μs; 1, 3, 7, 10, 15, 20, 30, and 80 ms. (f) Data for D85N/NG ($OD_{max} = 0.70$). Times after excitation: 50, 100, 150, 250, 500, 625, 750, and 880 ns; 1, 1.3, 1.5, 2, 5, 10, 25, 50, 75, 100, 200, and 400 μs; 1, 2, 4, 7, 10, and 20 ms. The singular values associated with the five largest basis spectra follow. For d-BR/NG: 4.479, 0.859, 0.276, 0.090, 0.057. For D96N/NG: 3.272, 0.502, 0.242, 0.179, and 0.056. For D85N/NG: 0.870, 0.688, 0.091, 0.049, and 0.021. For R82Q/NG: 1.122, 0.398, 0.093, 0.069, and 0.028.

(Miercke et al., 1991). p-BR is BR from the purple membrane of *H. halobium* that has been treated with papain before detergent solubilization and delipidation (Ross et al., 1989). The papain treatment gives a protein missing 17 amino acids on its C-terminus (Liao & Khorana, 1984). All these preparations (d-BR, e-BR, p-BR, and w-BR) had identical photocycles (results not shown). Neither the additional amino acids on the N-terminus, the removal of amino acids on the C-terminus, nor the denaturation, renaturation, and purification process affects the photocycle kinetics of monomeric BR.

Figure 1 shows the transient difference spectra for d-BR and the BR variants D85N, D96N, and R82Q in NG. Figure 2 contains the transient difference spectra for these BRs when they are solubilized in CHAPSO. Table I contains the observed lifetimes from the nonlinear fitting of these spectra.

d-BR. Since we have studied the photocycle of e-BR from mutants in detergent micelle preparations, it is important to understand the effect that this type of environment has on the photocycle of d-BR itself. Compared to PM, the wavelength of maximum absorbance is blue-shifted upon detergent solubilization. The λ_{max} values for d-BR in both NG and CHAPSO are 548 nm (dark-adapted, DA) and 555 nm (light-adapted, LA). Solubilizing BR in detergent also changes the

Table I: Lifetimes[a] from Global Fit

	lifetime for process					
	I	II	III	IV	V	ΣD^{2}[b]
d-BR/NG	0.69 μs	9.3 μs	2.0 ms	9 ms		0.0136 (0.010)
d-BR/CHAPSO	0.86 μs	10.2 μs	7.4 ms	70 ms	670 ms	0.0235 (0.012)
D96N/NG	0.35 μs	8.9 μs	0.13 ms	4.7 ms	100 ms	0.0177 (0.010)
D96N/NG, pH 6.5	0.35 μs	7.9 μs	0.11 ms	25 ms	170 ms	0.0124 (0.010)
D96N/CHAPSO	0.52 μs	4.7 μs	32 μs	47 ms	760 ms	0.057 (0.020)
D85N/NG[c]	0.51 μs	120 μs	6.5 ms			0.020 (0.012)
D85N/CHAPSO[c]	1.0 μs	130 μs	4.3 ms			0.0107 (0.008)
R82Q/NG[c]	0.59 μs	420 μs	9.3 ms			0.156 (0.011)
R82Q/CHAPSO	0.46 μs	5.0 μs	0.29 ms	4.9 ms	89 ms	0.0137 (0.010)

[a] Reproducibility of lifetimes for different samples under identical conditions is on the order of 10–20%; samples are at pH 5 unless otherwise indicated. [b] The final sum of the squared differences between the data and the fit is followed by a noise estimate in parentheses. [c] Blue form.

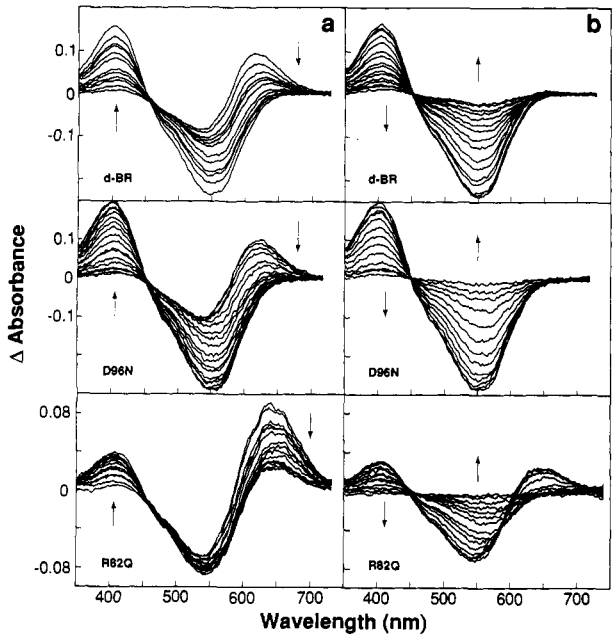

FIGURE 2: Transient difference spectra obtained for d-BR and preparations from mutants in CHAPSO after excitation at 532 nm with a 2-mJ, 7-ns laser pulse. (a) Short time data showing decay of KL and rise of M for (from top to bottom) d-BR/CHAPSO (OD_{max} = 0.85), D96N/CHAPSO (OD_{max} = 0.85), and R82Q/CHAPSO (OD_{max} = 0.70). Times after excitation for d-BR/CHAPSO: 50, 100, 250, and 500 ns; 1, 1.5, 3, 5, 7.5, 10, 15, 20, and 50 μs. For D96N/CHAPSO: 50, 100, 150, 250, 500, and 750 ns; 1, 1.5, 2, 3, 5, 7.5, 10, 15, 25, 35, 50, 100, and 250 μs. For R82Q/CHAPSO: 50, 100, 250, 350, and 750 ns; 1, 1.5, 3, 10, 50, 100, 150, 250, and 500 μs. (b) Long time data showing decay of M and return to the ground state for (from top to bottom) d-BR/CHAPSO, D96N/CHAPSO, and R82Q/CHAPSO. Times after excitation for d-BR/CHAPSO: 0.5, 1, 2.5, 5, 10, 20, 40, 80, 120, 200, 300, 500, and 750 ms; 1, 1.5, and 2 s. For D96N/CHAPSO: 0.25, 1, 3, 5, 10, 25, 50, 100, 200, 400, and 800 ms; 1.4, 2, and 4 s. For R82Q/CHAPSO: 0.5, 0.75, 1, 1.5, 3, 6, 10, 20, 40, 60, 80, 120, 200, 400, and 800 ms. The singular values associated with the five larges basis spectra follow. For d-BR/CHAPSO: 5.397, 0.883, 0.129, 0.061, and 0.038. For D96N/CHAPSO: 7.090, 1.164, 0.235, 0.153, and 0.0889. For R82Q/CHAPSO: 2.151, 0.661, 0.094, 0.069, and 0.028.

kinetics of the photocycle from those of BR in its native environment, the purple membrane (PM). Our recent studies on monomeric BR in six detergents discuss in detail the effect that different detergent environments have on the photocycle (Milder et al., 1991). The detergent environment changes the kinetics during both the rise and decay of the M intermediate. Most notably, the rise of M is faster and biphasic, and resembles the rise of M in PM at high pH. It seems that the interaction of the protein with detergent causes some conformational changes in the ground state of the protein, which perhaps result in the counterion moving closer to the Schiff base. Such an explanation is consistent with the blue-shifted absorption maximum of monomeric BR and the more rapid deprotonation/reprotonation kinetics in the L to M transition.

For d-BR/NG and d-BR/CHAPSO, the kinetics of the M rise are similar while the kinetics at later times are very different. Comparing the lifetimes in Table I and the intermediate spectra in Figure 3, it can be seen that the decay of M (processes III, IV, and V) is much slower and has one more exponential component in CHAPSO than in NG. The addition of this third relaxation of M to the fit for d-BR/CHAPSO is justified by a reduction of the final sum of squared residuals from 0.0429 to 0.0231. The residuals for d-BR/CHAPSO still show structure at long times, but adding one more relaxation to the fit does not reduce the final sum of residuals significantly. The fit for d-BR/NG gives residuals that are free from systematic structure. The slow M decay in d-BR/CHAPSO can be partly attributed to the more rigid environment in the CHAPSO micelles inhibiting a volume increase that must be necessary for the decay of the M and/or other of the later intermediates. This conformational change may be coupled to the effect of pH changes on the protonation states of residues in the protein. Note that the rise time of M is similar for BR in all the detergents that were studied and that it does not depend significantly on pH (Milder et al., 1991). This means that changes observed in the kinetics of the photocycle of e-BR from a site-directed mutant during the rise of the M intermediate can be attributed to the effect of the amino acid substitution with more confidence than changes during the later steps of the photocycle. After the formation of M, the effects of the solvation environment are greater (Fukuda et al., 1990; Milder et al., 1991), especially in the case of d-br/CHAPSO, where the effects of a mutation on the decay of the M intermediate are likely to be obscured by the effects of CHAPSO itself.

Asp-96 → Asn. D96N is perhaps the most studied mutant of BR, with previous kinetic studies emphasizing the role that Asp-96 plays in the decay of M. These studies have revealed a kinetic defect in the D96N photocycle which is characterized by the slowdown of the apparent decay of the M intermediate. In D96N, the M intermediate decays with an apparent rate that is linearly dependent on the proton concentration of the bulk solution. Interestingly, it has been shown that this defect can be overcome by the addition of small anions of weak acids, such as azide (Tittor et al., 1989). Some previous studies have concluded that the Asp-96 residue is directly involved in the reprotonation of the Schiff base in the M to N transition (Butt et al., 1989; Holz et al., 1989; Marinetti et al., 1989; Mogi et al., 1988; Otto et al., 1989; Tittor et al., 1989). These studies focused on the transient absorbance changes near 410 nm, where the M intermediate has its absorption maximum.

Transient changes at 410 nm will reflect the concentration of the M intermediate, but will not necessarily reflect solely

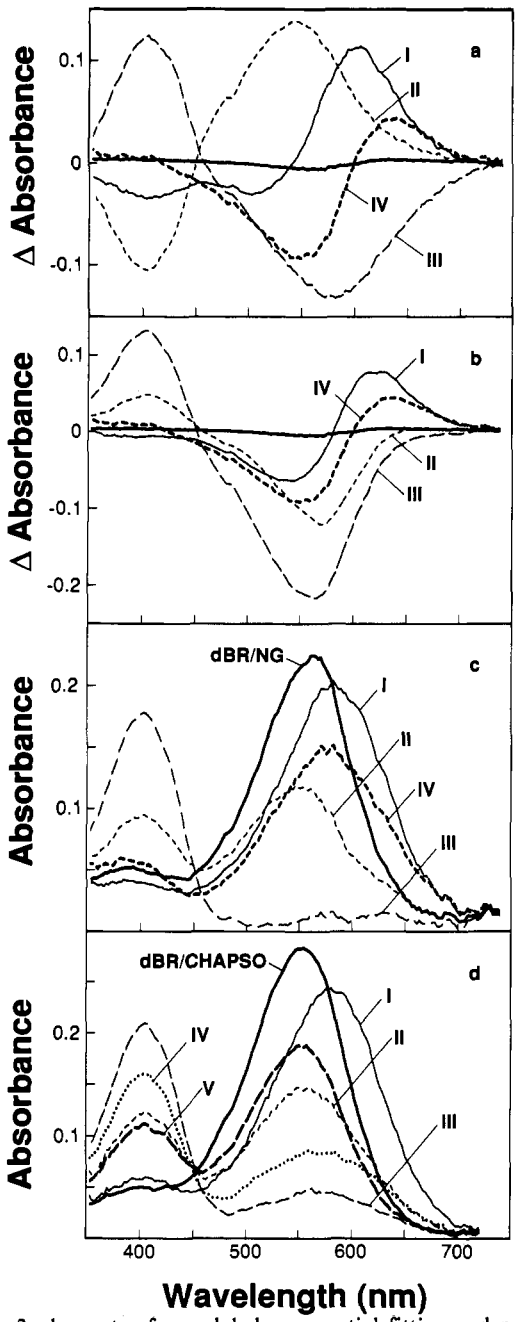

FIGURE 3: b-spectra from global exponential fitting and putative intermediate spectra calculated by assuming a simple sequential cycle for d-BR/NG and d-BR/CHAPSO. (a) b-spectra obtained after the SVD/nonlinear least-squares kinetic fit of the data shown in Figure 1a for d-BR/NG. The Roman numerals refer to the processes with apparent lifetimes that are given in Table I. (b) Difference spectra calculated from the lifetimes and b-spectra of the nonlinear least-squares fit assuming a purely sequential photocycle for d-BR/NG. (c) Putative intermediate spectra for d-BR/NG calculated by adding a scaled spectrum of light-adapted d-BR to the difference spectra shown in (b). (d) Putative spectra for the intermediates in the photocycle of d-BR/CHAPSO calculated by adding a scaled spectrum of light-adapted d-BR to the difference spectra calculated from the lifetimes and b-spectra from the nonlinear least-squares fit for d-BR/CHAPSO.

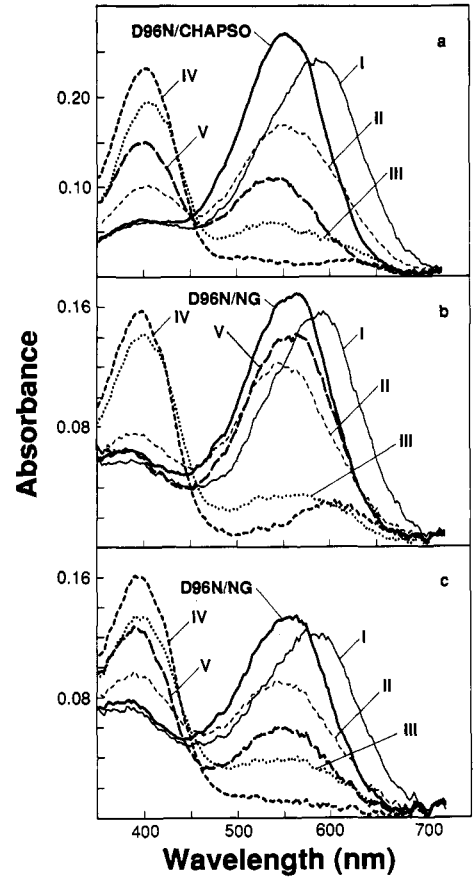

FIGURE 4: (a) Intermediate spectra for D96N/CHAPSO. (b) Intermediate spectra for D96N/NG, pH 5. (c) Intermediate spectra for D96N/NG, pH 6.5. All spectra are calculated from the global exponential fitting as in Figure 3.

the M to N process. For example, consider the putative mechanism M ⇄ N ⇄ O → BR, which is supported by recent kinetic absorption and resonance Raman measurements (Varo & Lanyi, 1990; Ames & Mathies, 1990). For a case where a biphasic decay of the concentration of M is observed, M will decrease until an equilibrium between it and later intermediates is established. Depending on whether a back-reaction occurs between N and O, this equilibrium will be between M and N or between M, N, and O. The second apparent decay of M will then actually reflect the kinetics of the N → O or O → BR reactions. A third phase may be possible if N → O is slower than O → BR. Clearly, the transient absorption decay at 410 nm can reflect other processes besides the M → N decay.

From the global fit, we have obtained spectra of the intermediates calculated from the b-spectra assuming a sequential pathway without any back-reactions (Figure 4). These spectra are informative despite the fact that the actual mechanism probably entails back-reactions, as these calculated spectra will reflect the concentrations of the different intermediates at equilibrium when the observed rates are well separated. In D96N/CHAPSO, the intermediate spectrum prior to the last decay (V in Figure 4a, τ = 760 ms) has peaks near 550 and 410 nm, indicating that the final decay is from an equilibrium mixture of M and N to BR. That O is not observed probably indicates that O → BR kinetics are much faster than those of N → O. Similar conclusions can be drawn from the intermediate spectra for D96N/NG (V in Figure 4b, τ = 100 ms). From these results, it can be concluded that an equilibrium between M and N is established, and that the slow rate is that of the N → O step in the photocycle. In this case, the apparent slow decay of the transient absorption around 410 nm is therefore due to the kinetics of the N → O reaction, rather than to slow M → N kinetics. For the photocycle of d-BR and D96N, the relative ratio of M and N when they are in equilibrium can be estimated from the ratio of the absorbances at 410 and 550 nm in the intermediate spectrum prior to the final decay (V in Figure 4). From this, it appears that the equilibrium contains more M in D96N than in d-BR. The

initial attainment of equilibrium is slower for D96N/NG at pH 6.5 (τ = 25 ms) than for D96N/NG at pH 5 (τ = 5 ms), as is the final decay (τ = 170 vs 100 ms). This slowdown is not observed for d-BR/NG in the pH range 5–7 (Milder et al., 1991). Thus, it appears that at least one equilibrium is reached between M and later photointermediates in D96N and that when the pH is increased both the rate for the attainment of this equilibrium and the rate of decay of the equilibrium mixture to BR are slowed down.

In the time regime from 50 ns to 500 μs, several interesting differences between the photocycles of d-BR and D96N are apparent in both detergent environments. First, the decay of KL (process I, Table I) is accelerated, with the L intermediate being formed about twice as fast in D96N as in d-BR. In addition, the M rise has a third kinetic component (process III, Table I) that is not found in the kinetics of d-BR. The intermediate spectra for the first two processes are similar to those for d-BR, but the lifetimes tend to be shorter (I and II in Figure 4 and Table I). The third rise of M has a lifetime of 32 μs in D96N/CHAPSO and 130 μs in D96N/NG. The addition of this relaxation to the fits for D96N is justified by a reduction in the final sum of squared residuals from 0.0409 to 0.0177 for D96N/NG at pH 5 and from 0.0392 to 0.0124 for D96N/NG at pH 6.5. Adding this relaxation removes the systematic structure that is seen in the residuals for the fit with four relaxations. The residuals for a four-exponential fit for d-BR/NG are without any significant structure, and adding one more relaxation reduces the sum of squared residuals by less than 10%. The third rise of M decreases the residuals from 0.088 to 0.057 for D96N/CHAPSO. The calculated spectra for the intermediates before and after this rise (assuming a simple sequential mechanism) show a small shift in the absorption maximum of the M intermediate (III and IV, Figure 4). Although this shift is only about 4 nm, it is within the wavelength resolution of the OMA and reproducible. We have not observed this effect in d-BR under our conditions. Note that resonance Raman studies of D96N/CHAPSO show the chromophore's LA ground-state vibrational spectrum is the same as in d-BR and that no differences were detected in the chromophore structure in the M intermediate between D96N/CHAPSO and d-BR (Lin et al., 1991).

Although our results indicate that in NG the D96N mutation slows down the rate of M decay and that the rate is pH-dependent, the decay is observed to be biphasic. On the basis of results from the study of M decay in HL vesicles, a model has been developed that predicts that M decay in D96N should be monophasic at all pHs (Otto et al., 1989). This prediction was based on the assumption that in this mutant the Schiff base is reprotonated directly from the cytoplasm in a bimolecular reaction since the normal internal proton donor is lacking. Assuming that Asp-96 is involved in the reprotonation pathway to the Schiff base, the biphasic decay of M in D96N in both CHAPSO and NG micelles may mean that Asp-96 is involved in the reprotonation of the Schiff base in an indirect manner, perhaps via another residue that then is reprotonated through an alternate path in the detergent micelles. If solvent accessibility to the chromophore in D96N is good, it is conceivable that a back-reaction from N to M might occur with proton exchange occurring strictly between the Schiff base and the medium. This would require a lowered pK for the Schiff base in the detergent samples as reprotonation directly from the medium *plus* a higher pK for the Schiff base than external pH would lead to monophasic kinetics.

Our results clearly show that substituting Asp-96 with Asn affects every step of the photocycle in NG micelles. This raises the question of whether D96N/NG has the same protein conformation as d-BR/NG. The observed third rise of M implicates involvement of Asp-96 in the process of M formation. The enhancement of the rate of KL decay suggests a role for this residue in L formation. One simple explanation consistent with all the results is that replacement of Asp-96 by Asn affects the conformation of the protein in a significant enough way such that the kinetics of all of the intermediate steps are affected. Conformational effects on protein function are always possible when site-specific mutagenesis is used. The mutation could render D96N more susceptible to pH-induced conformational changes that would lead to a different reprotonation pathway at high pH through, for example, direct protonation from the solvent. If the mutation leads to a more open structure in M, the enhancement of the rate of M decay by azide in D96N (Otto et al., 1989; Tittor et al., 1989) could be explained, as the small azide molecule would be able to diffuse all the way to the chromophore in the mutant but not in the wild type. The azide effect can, at high azide concentrations, lead to an even faster M decay than in the wild type. However, no enhancement of the rate of M decay upon addition of azide is detected in wild-type BR, perhaps implying that the chromophore is not as accessible to hydrogen azide during the photocycle of the wild type. Recent results on the structure of BR place Asp-96 at a distance of 10 Å from the chromophore (Henderson et al., 1990), making it unlikely that Asp-96 is the residue that directly protonates the Schiff base. Arg-227 → Gln (R227Q) has been shown to have a decreased rate of decay of its transient absorption around 410 nm, similar to the decrease in this rate for D96N (Stern & Khorana, 1989). It appears that R227Q has a similar kinetic defect as D96N, at least in regard to how it affects the later parts of the photocycle. Stern and Khorana (1989) discuss how Arg-227 and Asp-96 may form a salt bridge within the interior of BR, and it may be that disturbing this or some other structural feature leads to at least some of the kinetic changes observed in D96N.

Results from FTIR spectroscopy reported by different groups on D96N are in good agreement, but there is some disagreement regarding the interpretation of the data during the rise of the M intermediate. The negative/positive pair of peaks at 1742/1748 cm^{-1} has been assigned to the COOH vibrations of Asp-96, but the perturbations seen during the formation of the L and M intermediates are taken to signify either the deprotonation and subsequent reprotonation of Asp-96 or environmental changes near the residue. According to Braiman et al. (1988b), Asn-96 may be deprotonated as early as the L intermediate and is reprotonated again in M. However, Gerwert et al. (1989) explain the perturbations of the spectra in this time regime as resulting from conformational changes taking place near Asp-96 in the L intermediate, suggesting that the residue remains protonated until the decay of the M intermediate (Gerwert et al., 1989). If the observed changes in the kinetics seen in the early part of the photocycle can be attributed to processes in which Asp-96 is directly involved, then our results seem to favor the model proposed by Braiman et al. (1988b). Regardless of whether the conformational changes in the photocycle are characterized by de- and reprotonations of Asp-96 as early as in the KL → L transition, our results show that the kinetics of these changes are affected by replacement of Asp-96 by Asn.

The observed third kinetic rise of M can have a number of explanations. The possibility that there are many different forms of the M intermediate has often been suggested. Regardless of the mechanism for the formation of different forms of M, it is likely that they differ in protein conformation rather than in the state of the chromophore. The L, M, and N intermediates all have 13-cis configuration and are all characterized by an anti conformation around the carbon–nitrogen double bond (Ames et al., 1989; Fodor et al., 1988; Smith et al., 1984). Several studies indicate that protein structure changes occur during M (Glaeser et al., 1986; Gerwert et al., 1989, 1990). It has been suggested by Varo and Lanyi (1990) that at least two spectrally similar M species exist in sequence in the photocycle and that the $M_1 \rightarrow M_2$ step is irreversible. The observed blue-shift, associated with late M formation in D96N (compare III to IV and V in Figure 4), is most readily explained by such a presence of two different M intermediates. We therefore suggest that Asp-96 plays an active role in protein conformational changes that occur after the initial formation of M. Although this third rise of M is not observed in d-BR, it is possible that d-BR undergoes similar changes during its photocycle but that these changes are not resolved. If this is the case, these changes are not resolved either because the second and third processes have similar rates or because the spectral changes are obscured by the faster decay of the M intermediate.

The current results for the M decay in D96N/NG are different from previous results for this protein variant. The M decay is biphasic, whereas previous studies showed monophasic kinetics, and the M decay is faster than reported in PM (Miller & Oesterhelt, 1990) where the M decay lifetime is 241 ms at pH 5 and 1.3 s at pH 6.5. In the present case, the faster M decay is probably due to the effect of the detergent environment. Otto et al. (1989) also report M decay rates for D96N in DMPC/CHAPS mixed micelles that are greater than those reported for PM. Using the observed M to N decay lifetimes of 4.7 and 25 ms at pH 5 and 6.5, respectively, gives a slope of 0.5 for the pH dependence of log τ for M decay in D96N/NG. Otto et al. (1990) report a value of 0.8, and Miller and Oesterhelt (1990) find a slope of 0.5.

It has been shown that the specific detergent environment greatly affects the kinetics of the later intermediates in the photocycle of BR (Milder et al., 1991; Fukuda et al., 1990). Although we have documented these effects for d-BR, there is no guarantee that these effects will be comparable for the mutants. The large role that the environment plays is clearly demonstrated by comparing the kinetics of M decay for D96N in both detergent environments. At pH 5 in the NG micelles, the substitution causes a slowing of the M decay, whereas in CHAPSO the effects of the substitution on M decay are negligible. M decay in d-BR/CHAPSO is drastically slowed down compared to PM and is further slowed down with increasing pH. d-BR/NG, on the other hand, has an M decay rate that is similar to the one in PM, and it is not reduced with increasing pH in the pH range 4–7 (Milder et al., 1991). The effect that replacing Asp-96 with Asn has on the decay of the M intermediate in PM has been attributed primarily to a large change in the entropy of activation for the Schiff base reprotonation in D96N (Miller & Oesterhelt, 1990; Tittor et al., 1989). The reprotonation of the Schiff base is thought to be kinetically optimized by Asp-96 acting as a localized proton donor. In NG micelles, the role of Asp-96 as a localized proton donor may be less important, as the entropy barriers separating protein conformations in NG micelles could be different from those in the lattice of PM. While it is possible

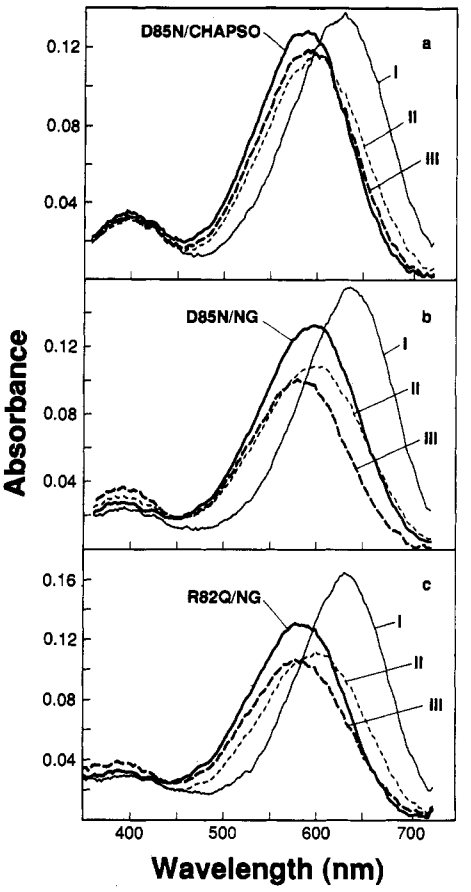

FIGURE 5: Spectra of the transient intermediates for the photocycles of the blue forms of D85N and R82Q obtained by adding back a portion of the light-adapted spectrum to the difference spectra calculated by assuming a simple sequential decay mechanism without back-reactions. (a) D85N/CHAPSO (b) D85N/NG. (c) R82Q/NG. Refer to Table I for the lifetimes of the intermediates.

that under our conditions the detergent environment rather than the D96N substitution is the most important factor in affecting the later steps of the photocycle, analysis of the difference spectra at earlier times clearly shows that the role of Asp-96 is not limited to the reprotonation of the Schiff base in the M → N step of the photocycle.

Asp-85 → Asn. Replacing Asp-85 with Asn abolishes the proton-pumping ability of BR (Mogi et al., 1988; Miercke et al., 1991). The ground-state absorption spectrum is red-shifted with a λ_{max} of 597 nm in NG and 583 nm in CHAPSO at pH 5 and shows no shift upon light-adaptation. The transient difference spectra of D85N show similar changes with time in both detergents (Figures 1, 2, and 5). The transient spectra, and the b-spectra resulting from the fit, show that an initially formed 640-nm-absorbing transient (I in Figure 5) decays into a 580-nm-absorbing intermediate (III in Figure 5) in two steps, with similar lifetimes in both detergents (Table I). Resonance Raman measurements on D85N/CHAPSO show that this intermediate (III) has a vibrational spectrum similar to that of the L intermediate in d-BR (Lin et al., 1991). This intermediate then decays in the millisecond time range. Spectra of these intermediates, shown in Figure 5, are calculated by assuming a simple sequential pathway and adding a scaled spectrum of the ground state. Studies, using single-wavelength measurements at 410 nm, have reported a transient absorption increase in the 100-μs time regime and attributed this to a delayed formation of M (Otto et al., 1990; Stern et al., 1989). The global analysis used here shows that this absorption increase at 410 nm can be explained by the third intermediate having a slightly higher extinction coefficient at 410 nm than

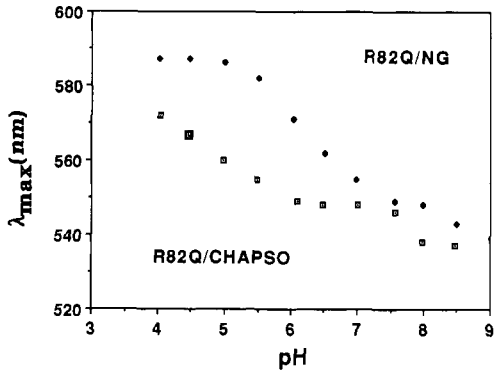

FIGURE 6: Absorption maxima (λ_{max}) in nanometers as a function of pH for dark-adapted R82Q/CHAPSO and R82Q/NG.

the intermediate preceding it, and thus its production is accompanied by a small increase in the transient absorption at 410 nm.

Our results support previous work that states that Asp-85 is a likely candidate for the primary counterion to the Schiff base in the light-adapted ground state of BR (Stern et al., 1989; Subramaniam et al., 1990; Otto et al., 1990). The absence of M in the photocycle also implies that this residue is involved in the deprotonation of the Schiff base in the L to M transition.

Arg-82 → Gln. We have observed that R82Q can be in either the blue and/or the purple form depending on pH and detergent environment. Figure 6 shows the pH dependence of the transition, as reflected in the observed λ_{max} of the dark-adapted form of the mutant, in both detergents. The transition from the purple to the blue form occurs at a lower pH in CHAPSO micelles than in NG micelles. The transition between the purple (~550 nm) and blue (~580 nm) forms of R82Q has a pK_a of about 5.5 in CHAPSO and about 6.5 in NG. The pK_a value in NG is closer to that observed in 1% DMPC/1% CHAPS/0.2% SDS (Stern & Khorana, 1989), and the lower value in CHAPSO may be due to a different surface to bulk pH ratio in the different detergent micelles. A transition to the blue form has been reported in PM when the pH of the solution is below 3 or after removal of all of the cations from the solution (Kimura et al., 1984; Muccio & Cassim, 1979; Szundi & Stoeckenius, 1989). Upon acidification of a solution of PM, a proton is taken up, suggesting that protonation of the counterion of the protonated Schiff base of retinal is occurring (Fischer & Oesterhelt, 1979). Alternatively, protonation of residues in the protein may be causing conformational changes near the chromophore (Szundi & Stoeckenius, 1989). Recent studies on the R82Q and related variants imply that protonation of Asp-85 regulates the purple to blue transition (Subramaniam et al., 1990). The blue form of R82Q, like D85N, is inactive in proton pumping (Subramaniam et al., 1990). The red shift in λ_{max} for R82Q upon light-adaptation is pH-dependent since it is affected by the relative amounts of the purple and blue forms. At pH 4 and 8, no red shift is observed upon light-adaptation, but the shift is 10 nm at pH 5–5.5 for R82Q/CHAPSO. Stern and Khorana (1989) reported the formation of a 490-nm absorber in R82Q upon prolonged illumination with red light. The lack of shift upon light-adaptation at pH 8 is not due to the formation of this species, but under our light-adaptation conditions, significant bleaching (40%) occurs in the purple form of R82Q/CHAPSO at pH 8.

Arg-82 is believed to be positioned near the retinal chromophore and has been suggested to be part of a complex counterion to the protonated nitrogen of the Schiff base that also involves Asp-85 and Asp-212 (Ames et al., 1990; Braiman et al., 1988b; Henderson et al., 1990; Lin & Mathies, 1989). Resonance Raman studies of R82Q/CHAPSO show a small shift of the C=NH$^+$ stretch in the light-adapted ground state, supporting this, but the M spectrum of R82Q/CHAPSO reveals no large differences with that of d-BR (Lin et al., 1991).

Figure 1 shows the transient difference spectra for the blue (R82Q/NG) form, and Figure 2 shows them for the purple (R82Q/CHAPSO) form of R82Q. The transient spectra for the blue form (R82Q/NG) are similar to those for D85N. The global analysis gives b-spectra and rate constants for R82Q/NG that are similar to those for D85N (Table I). The putative spectra, calculated by assuming a sequential pathway without back-reactions, show that the blue forms of R82Q and D85N have very similar photocycles (Figure 5). The λ_{max} for R82Q/NG at pH 5 is 585 nm, close to the λ_{max} of a solution of the pure, low-pH blue form (Figure 6).

To study the spectral/kinetic properties of the purple form, we used R82Q/CHAPSO at pH 5. The λ_{max} is 560 nm in the dark-adapted state (Figure 6) and shifts to 570 nm upon light adaptation. The transient difference spectra in Figure 2 show that an M intermediate is formed. Interestingly, the transient spectra show that the negative transient OD centered around 540 nm changes less during KL decay and M formation than in the case of d-BR. This indicates that transient accumulation of the L intermediate is less in the photocycle of R82Q than in the photocycle of d-BR and that most of the formation of M occurs upon decay of the KL intermediate. In addition to the normal photocycle intermediates the spectra show features attributable to the 13-cis form. This is reflected in the long-lived transient absorption around 650 nm which can be attributed to the C_{610} intermediate of a 13-cis photocycle. R82Q/CHAPSO at pH 5 also contains some of the blue form of the pigment, as can be seen on Figure 6. Therefore, in the case of R82Q/CHAPSO at pH 5, absorption of light will initiate at least three photocycles: the all-trans and 13-cis photocycles due to the purple form and the photocycle due to the blue form. In such a case where many photocycles occur in parallel, it is difficult to calculate intermediate spectra. Therefore, we present only the b-spectra in this case (Figure 7). In the photocycle for the cis form in PM, a red-absorbing species (C_{610}) is stable into the millisecond time regime (Hofrichter et al., 1989). In the results of our global analysis, C_{610} is represented by spectrum IV of the b-spectra (Figure 7). b-spectra I and II show the normal biphasic formation of M, with shorter lifetimes than for d-BR/CHAPSO. More than half of the M intermediate is formed concurrently with KL decay, as can be seen by comparing the amplitudes of b-spectra I and II in the wavelength region where M absorbs. In the case of d-BR, b-spectrum II looks like the L – M difference spectrum, as it represents the L → M transition (Milder et al., 1991). b-spectrum II for R82Q/CHAPSO has a much smaller amplitude in the spectral region where L normally absorbs, but has an additional positive component above 650 nm. The M formation in R82Q is thus faster than in d-BR and leads to much less transient accumulation of the L intermediates. The component above 650 nm in spectrum II indicates either a prolonged KL decay or a decay due to the blue form, as R82Q/CHAPSO at pH 5 contains some of the blue form (Figure 6). b-spectrum III shows a fast M decay with a lifetime of 0.3 ms, but most of the M decay is represented by b-spectrum V (τ = 90 ms). The presence of a 13-cis chromophore in the light-adapted state is supported by resonance Raman studies on R82Q/CHAPSO, as the vibrational spectra for the light-adapted ground state show that it contains

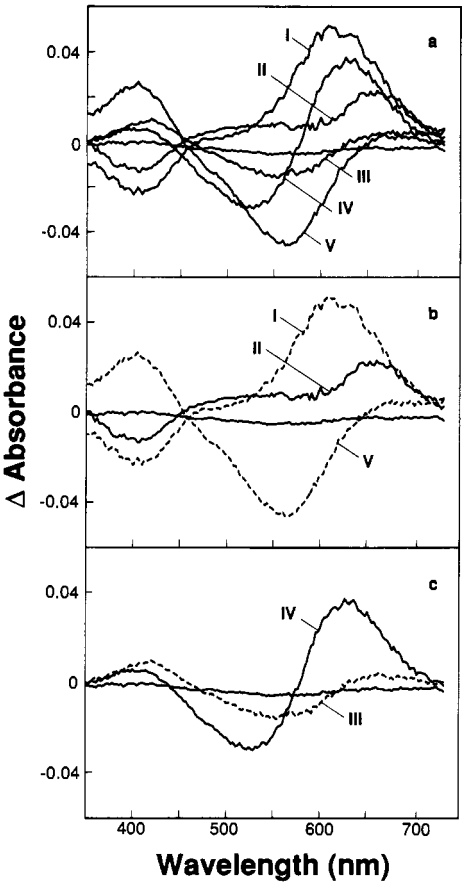

FIGURE 7: b-spectra from the nonlinear fit for R82Q/CHAPSO. (a) The b-spectra for R82Q/CHAPSO, pH 5. The Roman numerals refer to the processes with lifetimes in Table I. (b) The b-spectra primarily due to processes in the photocycle of the all-trans purple form of R82Q/CHAPSO; the b-spectra for processes I and II also have contributions from processes due to the blue form. (c) The b-spectra primarily due to processes in the photocycles of the 13-cis purple and the low-pH blue form of R82Q/CHAPSO; process IV represents the C_{610}-like intermediate in the photocycle of the 13-cis purple form, and process III can be attributed to the blue form, but may also contain a contribution from a fast-decaying M in the photocycle of the all-trans purple form.

13-*cis* and *all-trans*-retinal in equal proportions (Lin et al., 1991). This can also be seen from the relative amplitudes of the b-spectra, where spectrum IV represents the decay of the C_{610} intermediate in the 13-cis photocycle and spectrum V the decay of the M intermediate in the all-trans photocycle. The reduced proton-pumping efficiency of R82Q (Miercke et al., 1991; Stern & Khorana, 1989) can therefore be explained by its inability to light-adapt to the all-trans form. The presence of multiple photocycles in our R82Q/CHAPSO sample makes interpretation of the rapid phase of M decay difficult. The actual lifetime for the initial M decay cannot be extracted from the data since processes attributable to the photocycle of the blue form are occurring with similar rates (Table I). The second M decay (b-spectrum V) should not be contaminated by intermediates of the other photocycles, since decay of C_{610} and any intermediates resulting from the photolysis of the blue form is completed by the time scale of the second M decay. Thus, for R82Q, the purple form appears to have normal photocycle intermediates, though M both forms and decays faster than in d-BR/CHAPSO. The rapid formation of M, along with little transient accumulation of the L intermediate, supports the suggestion that Arg-82 is part of a complex counterion also involving Asp-85 and Asp-212 (Ames et al., 1990; Braiman et al., 1988b; Henderson et al., 1990; Lin & Mathies, 1989). When the positive charge of Arg-82 is absent, the counterion will have a more negative character, perhaps leading to a greater affinity for the Schiff base proton. That the decay of M is faster in the photocycle of R82Q than in d-BR may indicate a different decay mechanism for the M intermediate in R82Q. This has been suggested before, since previous work did not detect transient pH changes during the M decay of R82Q in 1% DMPC/1% CHAPS mixed micelles (Otto et al., 1990). However, the photocycle is clearly complex, and the mechanism may depend on the specific environment, as R82Q is observed to pump protons in vesicles, though with reduced efficiency (Miercke et al., 1991).

Conclusions

Our results support the previously proposed roles for Asp-85 and Arg-82 in BR and its photocycle (Stern et al., 1989; Subramaniam et al., 1990; Otto et al., 1990). M formation is blocked in the photocycles of the blue forms of R82Q and D85N, consistent with Asp-85 being the primary counterion of the protonated Schiff base of retinal and with Asp-85 being involved in the deprotonation of the Schiff base during M formation. The apparent pK_a for the purple to blue transition is increased upon removal of the positively charged Arg-82. This is readily explained with the complex counterion model, since the removal of the positively charged Arg-82 should cause an increase in the pK_a of Asp-85. Our results show that both M rise and M decay are accelerated in the purple form of R82Q. The faster rise can be explained by the greater affinity that the more negatively charged complex counterion will have for the Schiff base proton when the positive charge of Arg-82 is missing. The decay of M may be faster in R82Q due to an alteration of the reprotonation pathway that traps the Schiff base proton within the protein.

While our results for R82Q and D85N are consistent with previous studies, the improved time resolution of our spectra, combined with a global analysis of the data, leads to a more complex description of the role of Asp-96 than has previously been suggested. Analysis of the global kinetic fit for the photocycle of D96N shows that the rate of the M → N step is drastically reduced, with the rate of M decay more dependent on pH, relative to d-BR. This is consistent with the suggestion that Asp-96 donates the proton to the Schiff base in the M → N step. The observed biphasic decay of M may indicate that the reprotonation also involves another residue. However, the replacement of Asp-96 by Asn affects the rate of all the steps of the photocycle observed in this study. The formation of L is accelerated, and the formation of M has an additional slow component to the two observed in d-BR. Previous FTIR results show that the protein structure is slightly different for D96N vs BR in at least some of the intermediates. One interpretation of our results is that structural changes caused by replacing Asp-96 by Asn may lead to a different structure in the M intermediate, perhaps changing the apparent pK_a of residues involved in later steps of the photocycle and/or changing the accessibility of solvent to the chromophore in M. This would explain why the accelerating effect of azide on the apparent decay of the M intermediate is seen in D96N but not wild type. Such an effect on protein structure could be due to the formation or disruption of a salt bridge between Asp-96 and Arg-227 during the photocycle (Stern & Khorana, 1989). While the specific detergent environments used in this study may affect the later steps of the photocycle by changing the M decay in largely unknown ways, the results do show that the role of Asp-96 in the photocycle of BR is not limited to the reprotonation of the Schiff base in the M → N step of the photocycle and suggest that the residue may be important in the regulation of

structural changes in the protein.

References

Ames, J. B., & Mathies, R. A. (1990) *Biochemistry 29*, 7181–7190.

Ames, J. B., Fodor, S. P. F., Gebhard, R., Raap, J., van den Berg, E. M. M., Lugtenburg, J., & Mathies, R. A. (1989) *Biochemistry 28*, 3681–3687.

Braiman, M. S., Mogi, T., Stern, L. J., Hackett, N. R., Chao, B. H., Khorana, H. G., & Rothschild, K. J. (1988a) *Proteins: Struct., Funct., Genet. 3*, 219–229.

Braiman, M. S., Mogi, T., Marti, T., Stern, L. J., Khorana, H. G., & Rothschild, K. J. (1988b) *Biochemistry 27*, 8516–8520.

Butt, H. J., Fendler, K., Bamberg, E., Tittor, J., & Oesterhelt, D. (1989) *EMBO J. 8*, 1657–1663.

Chernavskii, D. S., Chizov, I. V., Lozier, R. H., Murina, T. M., Prokhorov, A. M., & Zubov, B. V. (1989) *Photochem. Photobiol. 49*, 649–653.

Duñach, M., Berkowitz, S., Marti, T., He, Y. W., Subramaniam, S., Khorana, H. G., & Rothschild, K. J. (1990) *J. Biol. Chem. 265*, 16978–16984.

Eisenstein, L., Lin, S., & Dollinger, G. (1987) *J. Am. Chem. Soc. 109*, 6860–6862.

Fischer, U., & Oesterhelt, D. (1979) *Biophys. J. 28*, 211–230.

Fodor, S. P. A., Ames, J. B., Gebhard, R., van den Berg, E. M., Stoeckenius, W., Lugtenburg, J., & Mathies, R. A. (1988) *Biochemistry 27*, 7097–7101.

Fukuda, K., Ikegami, A., Nasuda-Kouyama, A., & Kouyama, T. (1990) *Biochemistry 29*, 1997–2002.

Gerwert, K., Hess, B., Soppa, J., & Oesterhelt, D. (1989) *Proc. Natl. Acad. Sci. U.S.A. 86*, 4943–4947.

Gerwert, K., Hess, B., & Engelhard, M. (1990) *FEBS Lett. 261*, 449–454.

Glaeser, R. M., Baldwin, J., Ceska, T. A., & Henderson, R. (1986) *Biophys. J. 50*, 913–920.

Henderson, R., Baldwin, J. M., Ceska, T. A., Zemlin, F., Beckman, E., & Downing, K. H. (1990) *J. Mol. Biol. 213*, 211–230.

Hofrichter, J., Henry, E. R., & Lozier, R. H. (1989) *Biophys. J. 56*, 693–706.

Holz, M., Drachev, L. A., Mogi, T., Otto, H., Kaulen, A. D, Heyn, M. P., Skulachev, V. P., & Khorana, H. G. (1989) *Proc. Natl. Acad. Sci. U.S.A. 86*, 2167–2171.

Hug, S. J., Lewis, J. W., Einterz, C. M., Thorgeirsson, T. E., & Kliger, D. S. (1990) *Biochemistry 29*, 1475–1485.

Kimura, Y., Ikegami, A., & Stoeckenius, W. (1984) *Photochem. Photobiol. 40*, 641–660.

Lewis, J. W., Yee, G. G., & Kliger, D. S. (1987) *Rev. Sci. Instrum. 58*, 939–944.

Liao, M.-J., & Khorana, H. G. (1984) *J. Biol. Chem. 259*, 4194–4199.

Lin, S. W., & Mathies, R. A. (1989) *Biophys. J. 56*, 653–660.

Lin, S. W., Fodor, S. P. A., Miercke, L. J. W., Shand, R. F., Betlach, M. C., Stroud, R. M., & Mathies, R. A. (1991) *Photochem. Photobiol. 53*, 341–346.

Lozier, R. H., Bogomolni, R. A., & Stoeckenius, W. (1975) *Biophys. J. 15*, 955–962.

Marinetti, T., Subramaniam, S., Mogi, T., Marti, T., & Khorana, H. G. (1989) *Proc. Natl. Acad. Sci. U.S.A. 86*, 529–533.

Mathies, R. A., Brito Cruz, C. H., Pollard, W. T., & Shank, C. V. (1988) *Science 20*, 777–779.

Miercke, L. J. W., Stroud, R. M., & Dratz, E. A. (1989) *J. Chromatogr. 483*, 331–340.

Miercke, L. J. W., Betlach, M. C., Mitra, A. K., Shand, S., Fong, S. K., & Stroud, R. M. (1991) *Biochemistry 30*, 3088–3098.

Milder, S. J., & Kliger, D. S. (1988) *Biophys. J. 53*, 465–468.

Milder, S. J., Thorgeirsson, T. E., Miercke, L. J. W., Stroud, R. M., & Kliger, D. S. (1991) *Biochemistry 30*, 1751–1761.

Miller, A., & Oesterhelt, D. (1990) *Biochim. Biophys. Acta 1020*, 57–64.

Mogi, T., Stern, L. J., Marti, T., Chao, B. H., & Khorana, H. G. (1989) *Proc. Natl. Acad. Sci. U.S.A. 85*, 4148–4152.

Muccio, D. D., & Cassim, J. Y. (1979) *J. Mol. Biol. 135*, 595–609.

Nagle, J. F., Parodi, L. A., Lozier, R. H. (1982) *Biophys. J. 38*, 161–174.

Otto, H., Marti, T., Holz, M., Mogi, T., Lindau, M., Khorana, H. G., & Heyn, M. P. (1989) *Proc. Natl. Acad. Sci. U.S.A. 86*, 2228–9232.

Ottolenghi, M. (1982) *Methods Enzymol. 88*, 471–491.

Ross, P. E., Helgerson, S. L., Miercke, L. J. W., & Dratz, E. A. (1989) *Biochim. Biophys. Acta 991*, 134–140.

Rothschild, K. J. (1988) *Photochem. Photobiol. 47*, 883–887.

Rothschild, K. J., Braiman, M. S., He, Y. W., Marti, T., & Khorana, H. G. (1990) *J. Biol. Chem. 265*, 16985–16991.

Shand, R. F., Miercke, L. J. W., Mitra, A., Fong, S. K., Stroud, R. M., & Betlach, M. C. (1991) *Biochemistry 30*, 3082–3087.

Smith, S. O., Pardoen, J. A., Mulder, P. P. J., Curry, B., Lugtenburg, J., & Mathies, R. A. (1983) *Biochemistry 22*, 6141–6148.

Smith, S. O., Myers, A. B., Pardoen, J. A., Winkel, C., Mulder, P. P. J., Lugtenburg, J., & Mathies, R. A. (1984) *Proc. Natl. Acad. Sci. U.S.A. 81*, 2055–2059.

Stern, L. J., & Khorana, H. G. (1989) *J. Biol. Chem. 264*, 14202–14208.

Stern, L. J., Ahl, P. L., Marti, T., Mogi, T., Duñach, M., Berkowitz, S., Rothschild, K. J., & Khorana, H. G. (1989) *Biochemistry 28*, 10035–10042.

Stoeckenius, W., & Bogomolni, R. A. (1982) *Annu. Rev. Biochem. 51*, 587–616.

Subramaniam, S., Marti, T., & Khorana, H. G. (1990) *Proc. Natl. Acad. Sci. U.S.A. 87*, 1013–1017.

Szundi, I., & Stoeckenius, W. (1989) *Biophys. J. 56*, 369–383.

Tittor, J., Soell, C., Oesterhelt, D., Butt, H.-J., & Bamberg, E. (1989) *EMBO J. 8*, 3477–3482.

Varo, G., & Lanyi, J. K. (1990) *Biochemistry 29*, 2241–2250.

Xie, A. H., Nagle, J. F., & Lozier, R. H. (1987) *Biophys. J. 51*, 627–635.